Low magnetic susceptibility materials and applications in magnetic gradiometry

2009 Smart Mater. Struct. 18 095038

(http://iopscience.iop.org/0964-1726/18/9/095038)

Smart Mater. Struct. **18** (2009) 095038 (8pp) doi:10.1088/0964-1726/18/9/095038

Low magnetic susceptibility materials and applications in magnetic gradiometry

Andrew Sunderland[1], **Li Ju**[1], **David G Blair**[1], **Wayne McRae**[1,2] **and Howard Golden**[1,2]

[1] School of Physics, University of Western Australia, 35 Stirling Highway, Crawley WA 6009, Australia
[2] Gravitec Instruments, 35 Stirling Highway, Crawley WA 6009, Australia

E-mail: asund@physics.uwa.edu.au

Received 5 February 2009, in final form 6 July 2009
Published 10 August 2009
Online at stacks.iop.org/SMS/18/095038

Abstract
Magnetic gradiometers are powerful tools for mineral exploration. To avoid the problem of heading errors, gradiometers must be made from low susceptibility materials. We compare possible low susceptibility materials for gradiometer use and strategies for minimizing magnetic contamination. In particular, we present the favourable magnetic properties of the advanced engineering plastic Torlon.

1. Introduction

Newly introduced magnetic gradiometers could revolutionize airborne magnetic surveys. The gradient of the magnetic field can be used to interpret geological targets at depths up to several kilometres [1]. However, measurements would be biased by the presence of any magnetic material inside the gradiometer itself. Whereas magnetic fields from far field dipole sources scale as the inverse third power of distance, magnetic gradients scale as the inverse fourth power and are particularly sensitive to close objects.

There are many research groups developing magnetic gradiometers with different technologies: GETMAG [2] measures the magnetic gradient using a pair of SQuIDs, JESSY STAR [3] uses one SQuID that reads from two coils, Merayo *et al* [4] use a pair of fluxgate magnetometers, and various survey companies create a gradiometer by placing total field magnetometers on both wing tips of an aeroplane [5, 6]. The gradient is obtained by measuring the magnetic field at two locations and taking the difference.

A direct string magnetic gradiometer (DSMG) has been developed that employs a single aluminium 'string' as the sensing element [7]. Many DSMG instrument components are located near the long thin string where even small levels of magnetic contamination can lead to false signatures much larger than the signal from a distant geological target. These false signatures will manifest themselves as heading error.

McFee *et al* [8] define heading error as a systematic error that depends on the direction that the magnetic gradiometer is pointing relative to the direction of the Earth's magnetic field.

The magnetic field of the Earth induces material in the gradiometer to magnetize in the same orientation as the Earth's field. If the gradiometer is placed onboard a moving vehicle then those parts with induced magnetization will produce a magnetic gradient which varies whenever the vehicle changes direction. This variable error is a form of heading error.

For small magnetic fields, the induced magnetization $\mu_0\mathbf{M}$ of a material rises linearly with the applied magnetic field $\mu_0\mathbf{H} = \mathbf{B}_{\text{Earth}}$. When the vehicle carrying the gradiometer changes direction, the direction of $\mu_0\mathbf{H}$ will rotate in the magnetometer's reference frame but the magnitude of $\mu_0|H|$ will stay constant. The induced magnetization of each part can be predicted from the magnetic susceptibility $\chi = \frac{\partial \mathbf{M}}{\partial \mathbf{H}}$ and the heading of the vehicle. Using parts with low magnetic susceptibility will keep the total amount of heading error small.

Pure iron, nickel or cobalt materials are an obvious source of magnetic contamination. Other nonferrous metals of commercial grade are often less than 100% pure and usually contain iron as an impurity. Care must be taken when metals parts are used in a magnetic gradiometer because the susceptibility varies from alloy to alloy.

For these reasons, we report on the magnetic susceptibility of some common materials at room temperature. Section 2 describes the DSMG sensor and why it is particularly vulnerable to heading error. In section 3 we examine the materials used in this paper and why Torlon is important. Section 4 investigates the magnetic contamination caused by machining parts. We measure the susceptibility of each material before and after surface treatment. The magnetic

properties of an advanced engineering plastic Torlon are presented in detail (Torlon is used throughout the DSMG). Section 5 presents a study of the measurement uncertainties in this work. In conclusion, we aim to determine which materials are more suitable for use in the DMSG.

This work should also be of interest to all researchers working in the design and development of sensitive magnetic instrumentation because these devices require low magnetic susceptibility materials.

2. Direct string magnetic gradiometer

The DSMG detects magnetic gradients with only one sensing element, a long thin aluminium string. The string is clamped at both ends under tension with its second harmonic frequency approximately 800 Hz. An AC current sets the string into a resonant motion due to the magnetic force per unit length:

$$\frac{\partial \mathbf{f}}{\partial z} = i_s[\mathbf{e}_z \times \mathbf{B}]\sin(\omega t) \tag{1}$$

where $\mathbf{e}_z$ is a unit vector along the Z direction chosen to point along the string's length, i_s is the amplitude of the AC drive current, ω is the string's drive angular frequency, t is time and $\mathbf{B}$ is the magnetic induction vector.

We can tune the AC current frequency to the string's second harmonic frequency to create resonance. The string is a stretched thin flat ribbon so the resonant vibration only occurs in one direction. We can model the ribbon as a one-dimensional harmonic oscillator with an infinite number of resonant modes [9]:

$$\frac{\mathrm{d}}{\mathrm{d}t^2}X_n + \frac{2}{\tau}\frac{\mathrm{d}}{\mathrm{d}t}X_n + \omega_n^2 X_n = \left[\frac{2}{\pi n}(1-(-1)^n)B_y - (-1)^n\frac{2l}{\pi n}\frac{\mathrm{d}B_y}{\mathrm{d}z}\right]\frac{i_s}{\eta}\sin(\omega t). \tag{2}$$

From the above equation, the magnetic gradient term $\mathrm{d}B_y/\mathrm{d}z$ of the driving force couples to all resonant modes, while the conventional magnetic field term B_y is only coupled to the odd ones. Figure 1 shows the first two resonant modes of the DSMG.

This method of detection is insensitive to uniform magnetic fields. The 'S' shape of the second harmonic couples strongly to gradients but weakly to uniform fields. The resonance at the second harmonic will amplify magnetic gradient signals whilst the frequency is well off the first harmonic frequency that couples to the uniform magnetic field. Also, the mechanical displacement detection is designed to preferentially detect the second harmonic oscillations and suppress the fundamental mode oscillations. The high Q factor resonant structure of the string leads to a high common mode rejection that can be achieved without stringent balancing requirements [10].

Other magnetic gradiometers should not detect uniform magnetic fields however there is always a small but finite imbalance in the two sensing elements. Erroneous detection of uniform fields is another form of heading error. Careful calibration of the two sensing elements can be used to cancel out the heading error from magnetic parts. The DSMG is a single element device so this remedy is not available. The DSMG is particularly vulnerable to heading error.

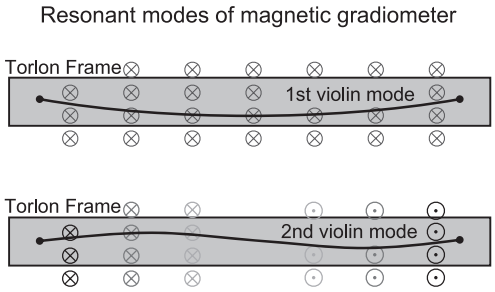

Figure 1. The top diagram shows the DSMG frame with the string clamped rigidly at each end. An AC current is running along the string such that its frequency is the same as the 1st violin mode of the string. Resonance will occur. The 'C' mode string vibrations will be sensitive to uniform magnetic fields (the magnetic field is shown going into the page). In the bottom diagram, the current has a frequency equal to the 2nd violin mode of the string. The 'S' mode string vibrations are sensitive to magnetic gradients.

3. Choice of low susceptibility materials

In this work we report on the laboratory materials: Torlon 4301, G10 Epoxy, machinable ceramic (Macor), Teflon (PTFE) and polyethylene terephthalate (PET). These are all non-magnetic materials that are suitable for magnetic detectors. The material Torlon 4301 is used throughout the latest DSMG. Macor, G10 and PTFE have been used in previous DSMGs.

The DSMG frame is made of Torlon 4301 (shown in figure 1) because Torlon's expansion coefficient is approximately the same as Aluminium 6061. An increase/decrease in temperature will loosen/stretch the string. In turn, the resonant frequency will shift and the level of $1/f$ noise will rise. This can be remedied by matching the thermal expansion coefficient of the frame to the aluminium string. A literature search by the authors found no magnetic susceptibility data for Torlon.

Most parts in magnetic instruments are made from non-magnetic plastics. Metals are potentially magnetic so they should be avoided where possible. However, some metal parts are required for their strength, electrical conductivity and thermal properties. In this work, we investigated aluminium 6061 because the DSMG's string is made of this material. We investigated oxygen free highly conductive copper (OFHC) because it is an excellent non-magnetic electrical conductor. We also investigated two brass alloys: yellow brass C27400 and leaded brass C33200. Although brass is known to be undependable in its magnetic properties [11], brass parts are still used in the construction of many magnetometers, e.g. [12–14].

We measured the susceptibility of all these materials with a view to reducing the heading error of the DSMG. Table 1 shows the concentration of ferromagnetic elements in each of the materials. The presence of iron impurities may increase the permeability of some of the materials. The results below show that this is the case, and also that surface contamination is a critical issue.

Table 1. Nominal concentrations were taken from material datasheets. The concentration of ferromagnetic elements in each sample were measured by the chemistry centre of Western Australia using a inductively coupled plasma—atomic emission spectrometer (ICP-AES).

	Nominal concentrations (ppm)			Measured concentrations (ppm)		
Material	Fe	Ni	Co	Fe	Ni	Co
Leaded brass	<3500	<4000	<5000	680	180	0.7
Yellow brass	<5000	<5000	<5000	1700	1500	7.5
Aluminium 6061	<7000	<5000	<5000	1700	45	0.1
OFHC copper	2	<1	<1	<5	1.3	<0.1
Torlon 4301:						
–Quadrant EPP				820	4	<1
–Ensinger				720	5	<1
G10				26	<0.2	<0.1
Macor				700	0	590
PTFE	<0.1	<0.1	<0.1	5	<0.2	<0.1
PET	<0.1	<0.1	<0.1	<5	<0.2	0.4

Table 2. The amount of mass lost by the rectangular metal samples in acid increases with longer immersion times. The uncertainty is ±0.01 g.

	Mass (g)			
Metal	As machined	After 10 min acid wash	After 70 min acid wash	After 24 h acid wash
Leaded brass	24.68	24.68	24.68	24.67
Aluminium	8.05	8.05	8.04	7.46

4. Comparison of materials and contamination reduction

4.1. Surface contamination

Ideally, the induced magnetization of a material is proportional to volume. However, there can also be a surface contamination from machining. Steel cutting tools will deposit iron onto the surface of the samples. This risk has been recognized in previous work [15–18], but has not been studied quantitatively. Here we do explore this problem quantitatively, before addressing the intrinsic properties of the samples.

Soft tools wear out quicker so they should emit more iron particles. We hypothesize that soft tools with high magnetic permeability should produce the most surface magnetic contamination. To investigate our hypothesis, 14 rectangular prism samples of 7 different materials were cut to dimensions 12 mm × 16 mm × 16 mm with a high carbon steel saw blade. Another 12 cylindrical samples of 6 different materials were machined with a high speed steel tool bit on the lathe to make cylinders of diameter 5 mm and length 5 mm. We drilled a 3 mm diameter hole into each cylinder and tapped the holes with a M3 tool steel tap. By testing both prisms and cylinders, we can compared the magnetic contamination from two different cutting motions.

To remove any surface magnetism, the metal prisms were immersed in 3% hydrochloric acid for durations of 10 min, 70 min, and 24 h. Corrosion of the samples prevented us from using a stronger acid. Table 2 shows that the aluminium sample lost 7% of its mass after being immersed in acid for 24 h.

Table 3 presents the susceptibility of the metal samples before and after an acid wash. The DSMG operates at room temperature so measurements were taken at room temperature. All susceptibility values in this paper are volume susceptibility in SI (MKS) units. A 24 h acid wash reduced the susceptibility of the metal prisms by an order of magnitude, although most of this reduction occurred in the first 10 min. The magnetic susceptibility that remains after 24 h could be produced by larger saw blade fragments that a weak acid can not remove. We conclude that a 10 min acid wash is an optimal compromise between contamination reduction and sample corrosion.

Washing the yellow brass sample in acid had no effect because the intrinsic susceptibility is so high that surface magnetic contamination is irrelevant.

The unwashed aluminium and leaded brass cylinders have susceptibilities that are much lower than their rectangular prism counterparts. This result can be explained by table 4, the relative permeability of the saw blade used to machine the rectangular prisms is much higher than the relative permeability of lathe tool bit and M3 tap used to machine the cylinders. The saw blade is also softer than the other tools so it should produce greater magnetic contamination according to our hypothesis.

We also investigated the magnetic contamination caused by steel scissors. After cutting 50 mm long, 0.125 mm diameter enamelled copper wire with steel scissors, the volume susceptibility was $2.9 \times 10^{-5} \pm 10^{-6}$. When the same wire was cut with a titanium side cutters, the volume susceptibility was only $5 \times 10^{-6} \pm 10^{-6}$.

Table 5 shows the magnetic susceptibility of the plastic and ceramic samples before and after a 24 h acid wash. In all cases the susceptibility was very low. The plastic and ceramic samples have much lower magnetic surface contamination than the metals samples. This result can be explained by the following background theory on machining.

In Atkin's and Liu's [19] model of ductile machining, the required cutting force will be greater for materials with a high toughness to strength ratio. Both macor and G10 have very low toughness and relatively high strength so these materials are not cut but grinded during machining. The brittle material will break in segmented chips [20] with an exceptional surface finish that is unlikely to contain impurities.

Table 3. The initial magnetic volume susceptibility of metals samples decreases after an acid wash, although most of the reduction occurs in the first 10 min of the acid wash. The prism samples were measured with a Bartington MS2b susceptibility meter. The cylindrical samples were measured using an Aerosonic 3001 vibrating sample magnetometer (VSM).

	Susceptibility, $\chi\,(10^{-5})$			
Metal samples	As machined	10 min acid wash	70 min acid wash	24 h acid wash
Prisms				
Leaded brass	2000 ± 300	180 ± 50	110 ± 50	
Aluminium 6061	1400 ± 400	250 ± 20	230 ± 20	230 ± 20
Cylinders				
Leaded brass	21 ± 5	9 ± 3		
Yellow brass	$20\,000 \pm 3000$	$20\,000 \pm 3000$		
Aluminium 6061	460 ± 100	17 ± 1		
OFHC copper	22 ± 4	2 ± 2		

Table 4. The permeability measurements were made with a Bartington MS2b susceptibility meter. The permeability of the tools varied ±30% when rotated. Hardness values are from a book by ASM International [33].

Tool	Material	Relative permeability	Hardness rockwell C
Lathe tool bit	High speed steel	1.4	64–65
M3 tap	Tool steel	3.7	61–62
Hacksaw blade	High carbon steel	11	59

Table 5. Initial magnetic volume susceptibility of plastic and ceramic samples before and after an acid wash. The prism samples were measured with a ZH Instruments SM-30 susceptibility meter. The cylindrical torlon samples were measured with a Quantum Design MPSM-7 SQuID.

	Susceptibility, $\chi\,(10^{-5})$	
Plastic and ceramic samples	As machined	24 h acid wash
Prisms		
Torlon 4301 (Quadrant EPP)	-1.7 ± 0.4	-1.9 ± 0.4
G10	0.8 ± 0.2	-0.1 ± 0.1
Macor	-0.6 ± 0.2	-0.8 ± 0.2
PTFE	-0.4 ± 0.1	-0.6 ± 0.2
PET	-0.5 ± 0.1	-0.7 ± 0.2
Cylinders		
Torlon 4301 (Quadrant EPP)	-1.1 ± 0.3	-2.1 ± 0.1
Torlon 4301 (Ensinger)	4.5 ± 0.5	0.57 ± 0.05

The three plastics Torlon 4301, PTFE and PET are soft materials with low coefficients of friction so the cutting force will be low according to Atkin's and Liu's model [19]. Both surface damage and tool wear will be minimal so contamination should be low.

Special precautions must be taken when machining OFHC copper in regards to cleanliness because of the great toughness of the material. Surface impurities may be ploughed under and entrapped during spinning operations on copper [21].

Work hardening of the surface during machining could also contribute to the change in susceptibility. Hutchison and Reekie [22] found that this was the case in copper and aluminium samples and that normal susceptibility could be restored by washing the samples in a weak nitric acid.

4.2. Intrinsic susceptibility of materials

The susceptibility of a sample after an acid wash should reflect the intrinsic susceptibility of the material. Table 6 presents the intrinsic susceptibility of every material in this paper. For aluminium and leaded brass, we measured the susceptibility of both cylinders and prisms, but only report the intrinsic susceptibility of the cylinders. The cylinder measurements are more reliable because they were exposed to less magnetic contamination. We were able to measure the susceptibility of Torlon EPP accurately for both prisms and cylinders, so the table reports an average of these two values.

We find that the non-metals are the least magnetic materials, all having magnetic susceptibilities on the order of 10^{-5}. G10 has the closest susceptibility to zero. In any case, the heading error caused by the plastic and ceramic parts will be negligible. Our results for macor and PTFE are in good agreement with the results of Keyser and Jefferts [23] whilst our result for PET agrees with Tanimoto *et al* [24]. Our measurement of G10's susceptibility is of the same order as Bossi *et al* s [25] who found traces of ferromagnetic impurities in commercial G10.

The susceptibility of OFHC copper is very low so it can be used for magnetic gradiometer parts that need to conduct electricity. There is however, a discrepancy between the magnetic susceptibility of OFHC copper $\chi \approx (2 \pm 2) \times 10^{-5}$ measured using the VSM and the textbook value of $\chi = -1 \times 10^{-5}$ [26]. This could be due to an imperfect acid wash or the limited precision of the VSM measurement.

The leaded brass, yellow brass and aluminium 6061 samples are intrinsically more magnetic than the other materials. These three metals are unsuitable for use in a magnetic gradiometer. There is a discrepancy between intrinsic susceptibility of aluminium 6061 $\chi \approx (17 \pm 1) \times 10^{-5}$ measured using the VSM and the susceptibility value reported by Keyser and Jefferts [23] $\chi = 1.9 \times 10^{-5}$. This could be due to different amounts of magnetic contamination between samples or an erroneous response of the Bartington MS2 to electrical conductivity (for example see Benech and Marmet [27]). In any case, aluminium 6061 is no longer used in the magnetic gradiometer (except for the string) because we wish to avoid any possible source of heading error.

Table 6. We present the intrinsic susceptibility of each material examined in this paper. All machined samples have been washed in acid. The right hand column notes the instrument used to make the susceptibility measurement.

Material	Intrinsic susceptibility $\chi\,(10^{-5})$	Instrument used
Metals		
Leaded brass	9 ± 3	VSM
Yellow brass	20000 ± 3000	VSM
Aluminium 6061	17 ± 1	VSM
OFHC Copper	2 ± 2	VSM
Plastics		
Torlon 4301 (Quadrant EPP)	-2.0 ± 0.1	SQuID/SM-30
Torlon 4301 (Ensinger)	0.57 ± 0.05	SQuID
G10	-0.1 ± 0.1	SM-30
Macor	-0.8 ± 0.2	SM-30
PTFE	-0.6 ± 0.2	SM-30
PET	-0.7 ± 0.2	SM-30
DSMG components		
Solder (60% tin, 40% lead)	0.05 ± 0.02	SQuID
Aluminized mylar tape	-2 ± 1	VSM
Printed circuit board	0 ± 1	VSM
Enamelled copper wire	0.5 ± 0.1	SQuID
Twist pair wire (Mogami 2490)	-0.2 ± 0.1	SQuID
Solid core wire (Brand Rex GT951007)	0.22 ± 0.05	SQuID

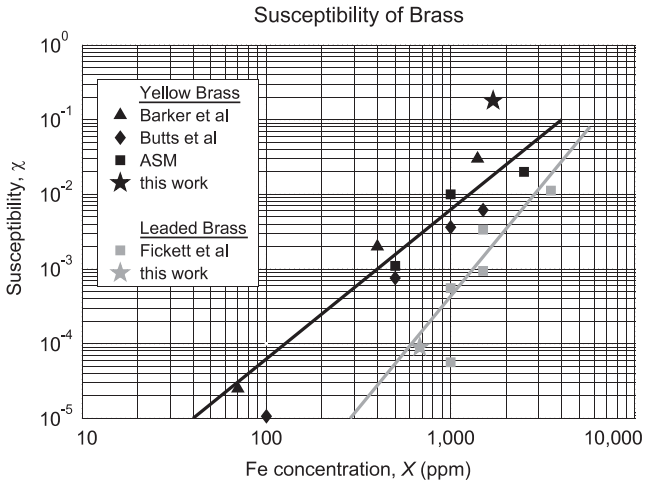

Figure 2. The susceptibility of brass rises rapidly with increasing iron concentration. The data is compiled from a paper by Barker *et al* [32], a paper by Butts *et al* [28], a book by ASM International [26], a paper by Fickett *et al* [11] and measurements performed by the authors on yellow and leaded brass samples. Barker and Butts measured the concentration of iron in their samples. For the data of ASM and Fickett, the graph plots the nominal concentration according to the UNS alloy number. The black line is a best fit for yellow brass at low Fe concentrations using a square law $\chi \propto X^2$. The grey line is a best fit for leaded brass.

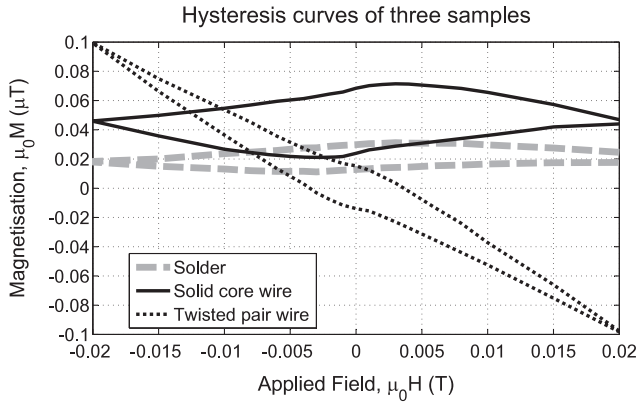

Figure 3. Magnetization of three non-magnetic materials that are used in the construction of the DSMG. The hysteresis loops start at $\mu_0 H = 0.02$ T, go down to $\mu_0 H = -0.02$ T and back to $\mu_0 H = 0.02$ T. Data taken using a Quantum Design MPSM-7 SQuID. Every time the hysteresis loops crossed $\mu_0 H = 0$, the MPSM's magnet was heated and reset in order to ensure there was no vortex trapping (vortex trapping could potentially cause a large H offset).

We compare the intrinsic susceptibility of the brass samples with the work of other researchers in figure 2. The graph plots volume magnetic susceptibility versus iron concentration for yellow brass (61–67% Cu, 33–39% Zn) and leaded brass (58–65% Cu, 33–40% Zn, 1–3% Pb). The results clearly show that the magnetic susceptibility χ of brass depends strongly on iron concentration X, the relationship is somewhere between $\chi \propto X^2$ and $\chi \propto X^3$ for low concentrations of iron. This leads to the general expectation that sample purity will often lead to variations in susceptibility in other copper alloys. However, there are other factors that affect the susceptibility of copper such as heat treatment [28], concentration of the iron impurity in small clumps [29], cold working and oxygen concentration [30]. The graph presents the susceptibility of brass as cast or as rolled because relying on a heat treatment to lower the susceptibility of a magnetic gradiometer is not sufficiently robust for all environments.

We also performed susceptibility measurements on a few non-standard wires and parts that are used in the DSMG, see figure 3. The bottom of table 6 shows that all of these materials have negligible magnetic susceptibility.

4.3. Torlon

Torlon 4301 is used throughout the DSMG so we did a thorough examination of its magnetic properties and compared

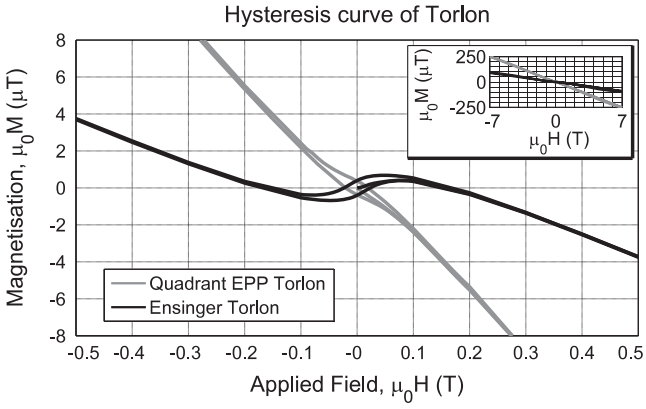

Figure 4. Magnetization of Torlon samples from two different manufacturers, taken after washing in acid for 24 h. The hysteresis loops start at $\mu_0 H = 0$, go up to $\mu_0 H = 7$ T (shown in inset), down to -7 T, and then back to 7 T. Data taken using a Quantum Design MPSM-7 SQuID.

two different manufacturers: Quadrant EPP and Ensinger. Figure 4 shows the magnetization $\mu_0 M$ of the acid washed Torlon cylinders as a function of the applied field $\mu_0 H$. The initial magnetic susceptibility of the Ensinger Torlon sample is positive $\chi = \frac{\partial M}{\partial H} = 6 \times 10^{-6}$. When the applied magnetic field exceeds $\mu_0 H > 0.1$ T, the magnetization has saturated and the volume susceptibility becomes negative $\chi = -1.3 \times 10^{-5}$. We conclude that Torlon is diamagnetic with some ferromagnetic impurities.

The entire magnetization curve of Ensinger Torlon exhibits hysteresis. The curve deviates from a straight line by $\Delta\mu_0 M = 2.4$ μT. In comparison, pure iron saturates at a magnetization of $\mu_0 M = 2.15$ T [31]. Assuming the ferromagnetic impurities are entirely Fe, the Ensinger and Quadrant EPP Torlon samples should contain 8 and 6 parts per million (ppm) Fe by mass respectively. Elemental analysis of both Torlon samples (shown in table 1) reveal a much higher concentration of iron, ~800 ppm Fe. This discrepancy could be due to the size and distribution of the iron particles affecting their magnetic ordering.

The SQuID results in table 6 show that the magnetic susceptibility of Torlon varies between the manufacturers. The cause of this variance is not clear since both samples have similar amounts of ferromagnetic impurities. Nevertheless, the initial magnetic susceptibility of the Quadrant EPP torlon cylindrical samples $\chi = -2.1 \times 10^{-5}$ are in good agreement with the Quadrant EPP rectangular samples $\chi = -1.9 \times 10^{-5}$.

5. Error analysis

Two samples of each material are used in this work. The difference between the two samples is a good estimate of the relative error. There is also core uncertainty contributions in the susceptibility apparatus that create absolute error. In this work, we used 4 different instruments to measure volume magnetic susceptibility:

- *Bartington MS2b susceptibility meter.* This instrument was used to measure the susceptibility of the 3 cm^3 metal prisms. The MS2b is designed for 10 cm^3 samples so the raw measurements were corrected using a formula by Dearing [34]. The susceptibility precision is $\pm 3 \times 10^{-5}$ for samples of this size. However, the metal prisms were highly contaminated and the difference between the 2 samples of the each material was greater than the error of the instrument in all cases.
- *ZH Instruments SM-30 susceptibility meter.* This was used to measure the susceptibility of the 3 cm^3 plastic and ceramic prisms. The SM-30 is designed for much larger samples so the raw measurements were corrected using a formula derived by Gattacceca *et al* [35]. The susceptibility precision of the instrument is $\pm 10^{-6}$ for samples of this size. We could not detect any difference between the 2 samples of each material. Gattacceca's formula has an uncertainty of $\pm 20\%$ and this is the main source of error for this instrument.
- *Aerosonic 3001 Vibrating Sample Magnetometer (VSM).* This instrument was used to measure the susceptibility of the metal cylinders, mylar tape and printed circuit board. The background susceptibility signal without any samples was $(1 \pm 1) \times 10^{-5}$. For the copper and brass samples, there was a significant difference between the susceptibility of the 2 samples of the same material. We added the sample error to the background error to get the uncertainty of these measurements.
- *Quantum Design MPSM-7 SQuID.* This was used to measured the susceptibility of the torlon cylinders and three different types of wire. The susceptibility was calculated by taking a linear fit of 11 evenly spaced magnetization measurements between $\mu_0 H = -0.01$ T and $\mu_0 H = 0.01$ T. The magnetization precision is $\Delta\mu_0 M = \pm 10$ nT. The error in the linear fit was added to the $\pm 5\%$ inaccuracy of the SQuID in order to get the total uncertainty of these measurements. There was also additional uncertainty in the susceptibility of the unwashed torlon cylinders because of the variation in the susceptibility between each pair of identical samples.

In order to predict the heading error of a magnetic gradiometer operating in the Earth's magnetic field, all of our susceptibility measurements were conducted in as low magnetic fields as possible. Weak signals make these measurements less precise than the results of other researchers. We could improve our precision by taking measurements in stronger magnetic fields and then extrapolating down to small fields, however extrapolating can be inaccurate because of hysteresis. The hysteresis loops in figure 3 show that hysteresis is a problem in commercial materials, even for materials that are only weakly magnetic.

The SQuID is the most accurate instrument out of the 4. However, the susceptibility meters have the advantage of taking measurements using very low applied fields, $\mu_0 H \ll 0.0001$ T. The MS2b and VSM have relatively low precision but they are sufficient to measure the susceptibility of the contaminated metal samples with better than 10% accuracy. The ZH Instruments SM-30 susceptibility meter is extremely precise for measuring the susceptibility of large samples such

as the plastic prisms. However, the SM-30 is not suitable for measuring metal samples which may be conductive.

The VSM utilized some custom built sample holders. We found that it had a small background susceptibility signal of $(1 \pm 1) \times 10^{-5}$. The other instruments were standard commercial devices and thus any background signals were either calibrated for or below the limits of detectibility.

6. Conclusion

We have investigated materials for use in high sensitivity magnetic gradiometers. We have shown that the material Torlon, which is a practical substitute for aluminium, has advantageous magnetic properties. The intrinsic susceptibility of Torlon 4301 varies between $\chi = 5.7 \times 10^{-6}$ and -2.1×10^{-5}, depending on the manufacturer. Other non-metals were shown to have low magnetic susceptibility $\chi \sim 10^{-5}$ and are suitable for use in sensitive magnetic instruments. OFHC copper also has low susceptibility, it can be used to make parts where the strength or conductivity of a metal is required.

Surface contamination had a large impact on the susceptibility of metal samples. Aluminium 6061 and leaded brass both have intrinsic susceptibilities on the order of $\chi \sim 10^{-4}$. Cutting the same materials with steel tools increased their susceptibility. Cutting with saw blades increased the susceptibility approximately one hundred fold to $\chi \sim 10^{-2}$, while machining with a lathe caused lesser contamination.

We found that washing metal parts in 3% hydrochloric acid for 10 min to be the optimal compromise between contamination reduction and sample corrosion. Washing the torlon cylinders in acid reduced the variation in susceptibility between samples. Washing the other plastic and ceramic samples in acid had negligible effect on their susceptibility which was already low.

Acknowledgments

The authors would like to thank Dr Alexey Veryaskin of Gravitec Instruments for many useful discussions and suggestions, A/Professor Tim St Pierre of the BioMagnetics and Iron BioMineralisation group at UWA for the use of the wet acid laboratory, Dr Robert Woodward and Mr Matt Carroll of the Biomagnetics Group at UWA for use of a MPSM-7 SQuID, Professor Li of the Tectonic Special Research Center at UWA for the use of a MS2b susceptibility meter, Mr Barry Price of the Chemistry Centre of WA for elemental analysis and Mr. Mads Toft of Alpha Geoscience for the use of a SM-30 susceptibility meter. Work on the DSMG project is funded in part by a linkage grant from the Australian Research Council.

References

[1] Schmidt P W and Clark D A 2000 Advantages of measuring the magnetic gradient tensor *Preview* **85** 26–30

[2] Schmidt P, Clark D, Leslie K, Bick M, Tilbrook D and Foley C 2004 GETMAG—A SQUID magnetic tensor gradiometer for mineral and oil exploration *Exploration Geophys.* **35** 297–305

[3] Stolz R, Zakosarenko V, Schulz M, Chwala A, Fritzsch L, Meyer H G and Kostlin E O 2006 Magnetic full-tensor SQUID gradiometer system for geophysical applications *The Lead. Edge* **25** 178–80

[4] Merayo J M G, Brauer P and Primdahl F 2001 Triaxial fluxgate gradiometer of high stability and linearity *Sensors Actuators* A **120** 71–7

[5] Killen P G 2006 Airborne geophysical surveying *Suppl. North. Miner* **92** 5–12

[6] Killen P G 2007 Airborne geophysical surveying *Suppl. North. Miner* **93** 6–15

[7] McRae W, Veryaskin A V, Ju L, Blair D G, Chin E, Dumas J and Lee B 2004 String magnetic gradiometer system: recent airborne trials *SEG Expand. Abstr.* **23** 790–3

[8] McFee J E, Bell M, Dempsey B, Chesney R H and Das Y 1985 A magnetostatic signature measurement and analysis system *J. Phys. E: Sci. Instrum.* **18** 54–60

[9] Veryaskin A V 2001 Magnetic gradiometry: a new method for magnetic *Sensors Actuators* A **91** 233–5

[10] Veryaskin A V 2009 Theory of operation of direct string magnetic gradiometer with proportional and integral feedback *Int. J. Appl. Electromagn. Mech.* **29** 197–215

[11] Fickett F R 1992 Low Temperature magnetic behavior of 'nonmagnetic' materials *Adv. Cryog. Eng.* **38** 1191–7

[12] Kobayashi K and Uchikawa Y 2003 Development of a high spatial resolution SQUID magnetometer for biomagnetic measurement *IEEE Trans. Magn.* **39** 3378–80

[13] Morello A, Angenent W G J, Frossati G and de Jongh L J 2005 Automated and versatile SQUID magnetometer for the measurement of materials properties at millikelvin temperatures *Rev. Sci. Instrum.* **76** 023902

[14] Bartington Instruments Mag-03MRN Three-Axis Magnetic Field Sensor http://www.bartington.com/products/Mag-03mrnthreeaxismagneticfieldsensor.cfm

[15] Spencer J F and John M E 1927 The magnetic susceptibility of some binary alloys *Proc. R. Soc.* A **116** 61–72

[16] Constant F W and Formwalt J M 1939 Investigation of ferromagnetic impurities I *Phys. Rev.* **56** 373–7

[17] Matsubayashi K, Maki M, Tsuzuki T, Nishioka T and Sato N K 2002 Magnetic properties (communication arising): parasitic ferromagnetism in a hexaboride? *Nature* **420** 143–4

[18] Wang W, Hong Y, Yu M, Rout B, Glass G A and Tang J 2006 Structure and magnetic properties of pure and Gd-doped HfO_2 thin films *J. Appl. Phys.* **99** 08M117

[19] Atkins A G and Liu J H 2007 Toughness and the transition between cutting and rubbing in abrasive contacts *Wear* **262** 146–59

[20] Society of Manufacturing Engineers 1996 *Materials Finishing and Coating* (*Tool and Manufacturing Engineers Handbook* vol 3) 4th edn, ed C Wick and R F Veilleux (Dearborn, MI: Society of Manufacturing Engineers) section 16-6

[21] Kohl W H 1995 *Handbook of Materials and Techniques for Vacuum Devices* (Woodbury, NY: America Institute of Physics) p 199

[22] Hutchison T S and Reekie J 1948 Strain sensitivity of magnetic susceptibility *Phys. Rev.* **73** 517–8

[23] Keyser P T and Jefferts S R 1989 Magnetic susceptibility of some materials used for apparatus construction (at 295 K) *Rev. Sci. Instrum.* **60** 2711–4

[24] Tanimoto Y, Fujiwara M, Sueda M, Sueda K, Inoue K and Akita M 2005 Magnetic levitation of plastic chips: applications for magnetic susceptibility measurement and magnetic separation *Japan. J. Appl. Phys.* **44** 6801–3

[25] Bossi I, Dilley N R, O'Brien J R and Spagna S 2004 Optimization of sample holder materials for sensitive magnetometry measurements at low temperatures *Mater. Res. Soc. Symp. Proc.* **825E** G5.5

[26] ASM International 2001 *ASM Specialty Handbook: Copper and Copper Alloys* ed J R Davis (Materials Park, OH: ASM International) p 487

[27] Benech C and Marmet E 1999 Optimum depth of investigation and conductivity response rejection of the different electromagnetic devices measuring apparent magnetic susceptibility *Archaeol. Prospect.* **6** 31–45
[28] Butts A 1954 *Copper: The Science and Technology of the Metal/its Alloys and Compounds* (New York: Reinhold Publishing) p 504
[29] Huck F B, Savage W R and Schweiter J W 1973 Magnetic susceptibility of α-phase Cu–Al and dilute magnetic Cu–Al(Fe) alloys *Phys. Rev.* B **8** 5213–20
[30] Ficket F R and Sullivan D B 1974 Magnetic studies of oxidized impurities in pure copper using a SQUID system *J. Phys. F: Met. Phys.* **4** 900–5
[31] Zhou S 1999 *Electrodynamics of Solids and Microwave Superconductivity* (New York: Wiley) p 90
[32] Barker J R 1948 The testing of brass and other constructional materials for ferromagnetic impurities *J. Sci. Instrum.* **25** 363–4
[33] ASM International 1982 *Engineering Properties of Steel* ed P Havrey (Materials Park, OH: ASM International)
[34] Dearing J A 1999 *Environmental Magnetic Susceptibility: Using the Bartington MS2 System* 2nd edn (Kenilworth: Chi Publishing)
[35] Gattacceca J, Eisenlohr P and Rochette P 2004 Calibration of *in situ* magnetic susceptibility measurements *Geophys. J. Int.* **158** 42–9